

The Conformations and Absolute Configurations of Two Preferred Diastereoisomers Having Composition $(\text{CH}_3\text{-C}_5\text{H}_4)\text{Mo}(\text{CO})_2[\text{HCPhR-N-C(Ph)-N-HCPhR}']$

MADELEINE DRAUX and IVAN BERNAL

Chemistry Department, University of Houston, University Park, Houston, Tex. 77004, U.S.A.

Received September 17, 1985

Abstract

The structure and absolute configurations of two compounds having composition $(\text{CH}_3\text{-C}_5\text{H}_4)\text{Mo}(\text{CO})_2[\text{HCPhR-N-C(Ph)-N-HCPhR}']$ were established by X-ray diffraction methods. MOC PME [R = CH₃, R' = H]: orthorhombic, space group $P2_12_12_1$; $a = 10.998(6)$, $b = 12.728(7)$, $c = 18.622(7)$ Å. $V = 2607$ Å³, $Z = 4$ molecules/unit cell. MOC P2 [R = CH₃, R' = CH₃]: triclinic, space group $P\bar{1}$; $a = 9.451(4)$, $b = 11.803(5)$, $c = 12.436(9)$ Å, $\alpha = 93.11(5)^\circ$, $\beta = 95.31(5)^\circ$, $\gamma = 100.06(5)^\circ$. $V = 1357$ Å³, $Z = 2$ molecules/unit cell. Both are thermodynamically preferred stereoisomers and as such show the typical conformation with the side phenyl rings facing the apical Cp. MOC PME has the absolute configuration (S; C)(R; Mo). MOC P2 bears optically active substituents at both benzamidine ligand nitrogens and is (S; C)(R; C). For MOC P2, asymmetry arises from the conformation of the molecule in the solid state but should average out in solution. The conformational effects of methylating the Cp were studied. A rationale is provided for the orientation of the phenyl rings with respect to the Cp ring, which does not appeal to packing forces.

Introduction

During the course of our studies of diastereoisomers having composition $(\eta^5\text{-C}_5\text{H}_5)\text{Mo}(\text{CO})_2$ (optically active thioamide) [1–3], we established three rules [4–7] that determine the preferred molecular conformations of the various diastereoisomers. These three rules, as follows, have also been applied successfully to the molecular conformations of another class of compounds, the molybdenum benzamidines [4, 6, 8] depicted in Fig. 1.

1. The C–H bond on the carbon β to the metal lies in the ligand plane (defined by N–C–N) with H away from the metal.

2. The interaction between a side chain phenyl and the Cp is slightly attractive.

3. The interaction between a side chain alkyl group and the Cp is slightly repulsive, and forces

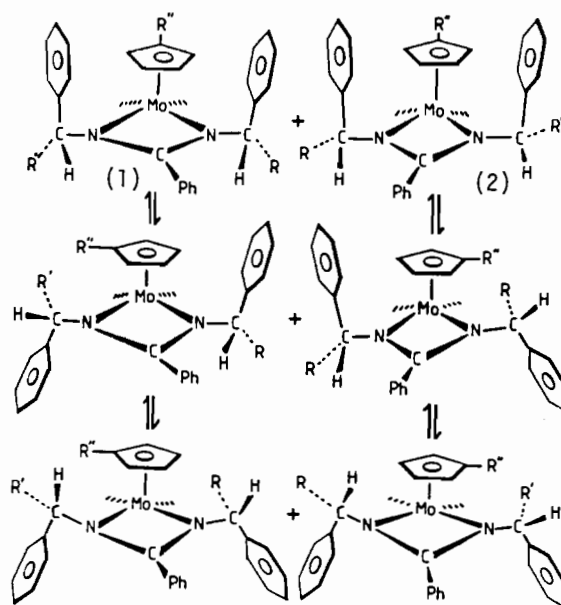


Fig. 1. Possible stereoisomers in Mo-Benzamidine Series.

the C–H bond slightly away from its preferred position in the ligand plane.

These rules can be applied not only to chiral substituents such as $\text{CH}(\text{CH}_3)(\text{C}_6\text{H}_5)$, but also to groups such as $\text{CH}_2\text{C}_6\text{H}_5$ or $\text{CH}(\text{CH}_3)_2$. Figure 1 shows the possible diastereoisomers of the Mo-benzamidine series in their preferred conformations. Equilibrium between those various stereoisomers has been studied in solution [5, 7, 9, 10] and it has invariably been found, in the thioamide and benzamidines series, that the preferred diastereoisomer (*i.e.*, the major species in solution) is the one having the side phenyls facing the Cp ring, as illustrated by (1) and (2) in Fig. 1. For example, in the following equilibrium [7] the molar ratio (IIa/IIb) is 6/94.

We now report the structure of two new benzamidines having a methylated Cp ring. Hereafter, we will refer to the two species described in this report by the following abbreviations:

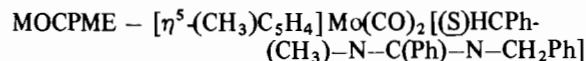
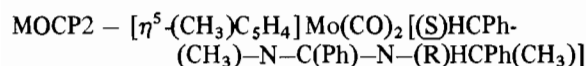
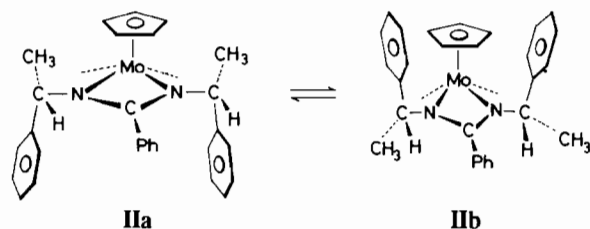


TABLE I. Summary of Data Collection and Processing Parameters

	MOC PME	MOC P2
Space group	$P2_12_12_1$	$P\bar{1}$
Cell constants	$a = 10.998(6)$ Å $b = 12.728(7)$ Å $c = 18.622(7)$ Å $\alpha = \beta = \gamma = 90^\circ$	$a = 9.451(4)$ Å $b = 11.803(5)$ Å $c = 12.436(9)$ Å $\alpha = 93.11(5)^\circ$ $\beta = 95.31(5)^\circ$ $\gamma = 100.06(5)^\circ$
Cell volume	2607 Å ³	1357 Å ³
Molecular formula	$\text{MoO}_2\text{N}_2\text{C}_{30}\text{H}_{28}$	$\text{MoO}_2\text{N}_2\text{C}_{31}\text{H}_{30}$
Molecular weight	544.51 g/mol	558.54 g/mol
Density (calc; $Z = 4$)	1.387 g/cm ³	
Density (calc; $Z = 2$)	—	1.367 g/cm ³
Radiation	Mo $K\alpha$ ($\lambda = 0.71073$ Å)	
Absorption coefficient	4.62 cm ⁻¹	4.45 cm ⁻¹
Data collection range	$4^\circ \leq 2\theta \leq 55^\circ$	
Scan width	$\Delta\theta = (1.00 + 0.35 \tan \theta)^\circ$	
Maximum scan time	180 s	
Scan speed range	0.5 to 3.35 deg/min	
Total data collected	3380	6330
Data with $I > 3\sigma(I)$	1756	
Data with $I > 4.5\sigma(I)$		3938
Total variables	152	300
$R = \sum \ F_o - F_c\ / \sum F_o $	0.036	0.056
$R_w = [\sum w^2(F_o - F_c)^2 / \sum w^2 F_o ^2]^{1/2}$	0.031	0.051
Weights		$w = [\sigma(F_o)]^{-2}$
Goodness of fit	0.99	2.83



Both compounds are preferred diastereoisomers. MOC PME and the previously reported Benz I [8] differ only the fact that in the former the Cp ring is methylated. The object of methylating the Cp ring is to restrain it from free rotation, as observed in solution [10]. We wanted to probe the effect, if any, of methylating the ring upon the equilibria between preferred and non-preferred diastereoisomers and determine what stereochemical effects, if any, such a substitution would cause. In this paper, we will concentrate on the information given by the crystal structure determination, and especially on the interaction between the side phenyl ring and the Cp ring.



Experimental

Similar methods were used for the two compounds. Intensity measurements were made on an ENRAF-NONIUS CAD-4 computer controlled diffractometer with Mo $K\alpha$ radiation monochromatized by a dense graphite crystal assumed for all purposes to be ideally imperfect. A summary of the crystallographically important parameters for data collection and processing are given in Table I. From the systematic absences noted the space groups were shown to be $P2_12_12_1$ (MOC PME) and $P1$ or $P\bar{1}$ (MOC P2). Three standard reflections were monitored every two hours during the course of data collection as a check of crystal stability and never showed any significant deviation from the initial measurements. In reducing the data, Lorentz and polarization factors were applied, but no absorption correction was made. A three dimensional Patterson map was computed and the position of the molybdenum atom was determined. All the remaining non-hydrogen atoms were found from successive difference Fourier maps and refined. Details of the refinement specific to each compound are given in parts (a) and (b) below. The atomic scattering factors for the non-hydrogen atoms were computed from numerical

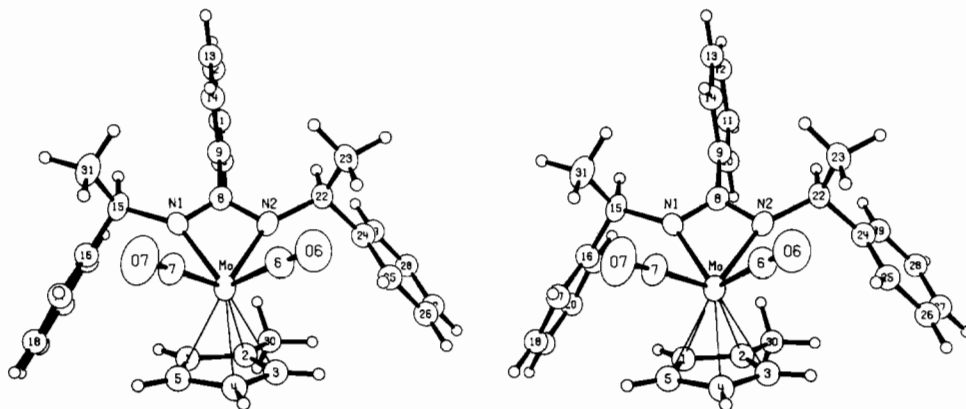


Fig. 2. Stereoscopic view of the molecule of MOCP2 showing the atom labelling scheme.

TABLE II. Determination of the Absolute Configuration of MOCPME

Reflection number	Indices	$F(\text{calc.})$ (hkl)	$F(\text{calc.})$ ($\bar{k}\bar{k}\bar{l}$)	Calc. F^a ratio	Meas. F^b ratio
1	4 3 12	181	192	0.943	1.050
2	1 2 6	258	240	1.075	0.928
3	5 1 6	224	236	0.949	1.063
4	3 1 1	234	216	1.083	0.908
5	4 1 16	249	240	1.038	0.970
6	3 1 16	255	266	0.959	1.049
7	3 4 13	299	289	1.035	0.962
8	7 4 13	201	209	0.962	1.038
9	4 5 13	288	278	1.036	0.963
10	3 7 10	259	269	0.963	1.041
11	3 6 6	237	247	0.960	1.028
12	1 10 2	237	227	1.044	0.962

^aCalc. $F(hkl)/\text{Calc. } F(\bar{k}\bar{k}\bar{l})$. ^bMeas. $F(hkl)/\text{Meas. } F(\bar{k}\bar{k}\bar{l})$.

Hartree–Fock wave functions [11]. For hydrogens, those of Stewart *et al.* [12] were used. The anomalous dispersion coefficients of Cromer and Liberman [13] were used for molybdenum.

(a) Details of the Refinement for MOCPME

Except for the phenyl and cyclopentadienyl groups, all non-hydrogen atoms were refined anisotropically, with hydrogen atoms added at theoretical positions (C–H 1.08 Å) on the methyl groups. The three phenyl groups and the methylcyclopentadienyl ring were refined as rigid bodies with idealized hydrogens. At this stage, the image of a second cyclopentadienyl appeared in the difference map, displaced with respect to the first one. (All atomic coordinates were then reversed after the absolute configuration determination: see next paragraph). The thermal parameters and occupancy factors of the two rings were refined in alternate cycles, with the thermal parameters constrained to be the same for the two rings. The two rings did not coalesce, the occupancy factor

refined to 80%, and the R factor improved. Further refinement yielded the agreement factors listed in Table I. The highest residual electron density was $0.4 \text{ e}^-/\text{Å}^3$, in the region of the phenyl rings. The only high correlations occurred between parameters within some of the rigid groups, and they were all less than 70%.

Determination of the absolute configuration

When refinement first converged, the molecular configuration was the mirror image of that given in Fig. 2. Structure factor tables were computed using the two possible configurations (x, y, z and $\bar{x} \bar{y} \bar{z}$) and a set of 12 reflections (Table II) was chosen for which the two Friedel pairs showed marked differences. Each of the 12 reflections was measured four separate times and the results averaged. They consistently showed [14] that the correct absolute configuration was the mirror image of the refined enantiomer, chosen during the initial solution of the structure. The absolute configuration thus

TABLE III. Atomic Coordinates and Thermal Parameters ($\times 1000$, for Mo $\times 10^3$) for MOC₂P₂

Atom	x/a	y/b	z/c	U_{11}	U_{22}	U_{33}	U_{12}	U_{13}	U_{23}
Mo	0.35567(8)	0.24405(6)	0.84894(6)	382(4)	388(4)	458(4)	10(3)	22(3)	23(3)
O6	0.3352(6)	0.4967(5)	0.9165(5)	87(5)	54(4)	104(5)	21(4)	12(4)	-11(4)
O7	0.0538(6)	0.2497(6)	0.9247(5)	58(4)	122(6)	108(6)	5(4)	33(4)	-10(4)
N1	0.2509(6)	0.1616(5)	0.6962(4)	37(4)	39(4)	41(4)	3(3)	6(3)	11(3)
N2	0.4261(6)	0.3039(5)	0.6973(4)	38(4)	42(4)	41(4)	-2(3)	-2(3)	1(3)
C6	0.3442(8)	0.4038(7)	0.8854(7)	34(5)	54(6)	97(7)	16(4)	3(4)	21(5)
C7	0.1604(10)	0.2468(8)	0.8933(7)	34(6)	43(6)	48(6)	5(5)	17(5)	-10(5)
C8	0.3274(7)	0.2273(6)	0.6339(6)	38(4)	39(4)	47(5)	12(4)	2(4)	-3(4)
C9	0.3103(8)	0.2192(6)	0.5152(6)	39(5)	41(5)	43(5)	-7(4)	6(4)	-2(4)
C10	0.3958(9)	0.1639(7)	0.4555(7)	54(6)	57(6)	67(6)	-8(4)	15(5)	-15(5)
C11	0.3741(11)	0.1574(8)	0.3431(8)	73(8)	84(8)	77(8)	-23(6)	33(6)	-30(6)
C12	0.2679(13)	0.2059(10)	0.2915(8)	92(9)	117(10)	46(7)	-68(8)	20(6)	-12(6)
C13	0.1850(10)	0.2637(8)	0.3501(8)	66(7)	77(7)	65(7)	-24(5)	-6(6)	13(6)
C14	0.2066(9)	0.2699(7)	0.4613(7)	57(6)	56(6)	53(6)	-8(5)	9(5)	2(5)
C15	0.1344(8)	0.0630(6)	0.6495(6)	40(5)	44(5)	49(5)	-8(4)	0(4)	-6(4)
C16	0.1521(8)	-0.0451(7)	0.7022(7)	33(5)	44(5)	63(6)	-11(4)	-4(4)	1(4)
C17	0.1090(9)	-0.0695(9)	0.8028(8)	58(6)	78(7)	81(7)	-27(5)	-11(5)	13(6)
C18	0.1335(12)	-0.1734(11)	0.8503(10)	75(8)	101(10)	100(10)	-43(7)	-19(7)	30(8)
C19	0.2033(14)	-0.2458(11)	0.7956(12)	100(11)	71(9)	138(14)	-33(7)	-46(10)	30(9)
C20	0.2418(11)	-0.2256(9)	0.6964(11)	76(8)	58(8)	170(13)	11(6)	-31(9)	-12(8)
C21	0.2190(9)	-0.1227(8)	0.6501(8)	49(6)	53(6)	113(8)	-5(5)	-3(5)	-3(6)
C22	0.5072(8)	0.4046(7)	0.6495(6)	54(5)	49(5)	35(5)	-13(4)	-2(4)	5(4)
C23	0.4399(8)	0.5106(6)	0.6578(7)	54(6)	41(5)	92(7)	0(4)	-6(5)	22(5)
C24	0.6666(9)	0.4277(6)	0.6962(7)	57(6)	30(4)	61(6)	-8(4)	8(5)	7(4)
C25	0.7091(9)	0.4763(7)	0.7999(7)	56(6)	55(6)	71(6)	-10(4)	-2(5)	11(5)
C26	0.8550(12)	0.4982(8)	0.8425(9)	72(8)	67(7)	121(10)	-21(6)	-31(7)	22(6)
C27	0.9556(13)	0.4694(10)	0.7845(14)	50(8)	75(10)	239(19)	-8(7)	12(11)	39(10)
C28	0.9176(13)	0.4231(10)	0.6788(13)	72(10)	65(8)	231(18)	11(7)	67(10)	24(9)
C29	0.7711(11)	0.3992(7)	0.6334(8)	72(7)	57(6)	120(9)	-5(5)	37(7)	-5(6)
C31	-0.0139(8)	0.0972(7)	0.6558(7)	40(5)	60(6)	96(7)	-2(4)	-5(5)	2(5)
C1	0.4470(5)	0.0706(3)	0.8867(4)	57(2)					
C2	0.5682(5)	0.1569(3)	0.8742(4)	61(2)					
C3	0.5738(5)	0.2478(3)	0.9550(4)	60(2)					
C4	0.4561(5)	0.2177(3)	1.0173(4)	73(3)					
C5	0.3777(5)	0.1081(3)	0.9751(4)	70(3)					
C30	0.6793(5)	0.1492(3)	0.7933(4)	80(3)					
H15	0.1398(56)	0.0486(45)	0.5619(45)	34(17)					
H22	0.5033(49)	0.3896(39)	0.5746(38)	6(14)					
H23A	0.4344(8)	0.5382(6)	0.7413(7)	92(9)					
H23B	0.3320(8)	0.4812(6)	0.6184(7)	92(9)					
H23C	0.4931(8)	0.5821(6)	0.6170(7)	92(9)					
H30A	0.7600(5)	0.2271(3)	0.8027(4)	92(9)					
H30B	0.6250(5)	0.1396(3)	0.7121(4)	92(9)					
H30C	0.7308(5)	0.0758(3)	0.8075(4)	92(9)					
H31A	-0.0305(8)	0.0979(7)	0.7405(7)	92(9)					
H31B	-0.0863(8)	0.0252(7)	0.6119(7)	92(9)					
H31C	-0.0352(8)	0.1767(7)	0.6242(7)	92(9)					

obtained shows C22 in an (S) configuration. Using the extension of R₂S system [15] to polyhapto ligands in organometallic complexes [16], the priority sequence of the ligands is C₅H₅ > N2 > N1 > CO. Thus the configuration at the Mo atoms is (R).

(b) Details of the Refinement for MOC₂P₂

The two molecules in the unit cell were found to be related by a center of symmetry, indicating a $P\bar{1}$

space group. The cyclopentadienyl and phenyl rings were first refined as rigid bodies, but a second image of each phenyl ring appeared, only slightly displaced with respect to the first one. The isotropic, rigid body model being thus found to be inadequate it was set aside and all phenyl rings carbons were made anisotropic. After all shifts/e.s.d.s were less than 0.1, the refinement converged to the agreement factors listed in Table I.

TABLE IV. Atomic Coordinates and Thermal Parameters ($\times 1000$) for MOC PME

Atom	x/a	y/b	z/c	U_{11}	U_{22}	U_{33}	U_{12}	U_{13}	U_{23}
Mo	0.55029(6)	0.88980(5)	0.97115(3)	464(3)	600(3)	453(3)	1(5)	68(4)	-40(5)
O1	0.5286(6)	0.6478(4)	0.9583(3)	130(5)	63(4)	94(4)	-28(4)	26(5)	-10(4)
O2	0.6773(6)	0.8020(5)	1.1067(3)	130(6)	102(5)	56(4)	31(5)	-9(4)	11(4)
N1	0.7197(5)	0.9727(4)	0.9604(3)	51(4)	57(4)	49(4)	-13(3)	6(4)	-19(4)
N2	0.6482(5)	0.8905(5)	0.8687(3)	49(4)	65(4)	46(3)	0(4)	10(3)	-12(4)
C6	0.5390(8)	0.7387(6)	0.9614(4)	74(5)	70(5)	55(5)	-20(6)	10(6)	-3(5)
C7	0.6307(7)	0.8337(6)	1.0552(4)	73(6)	59(6)	51(5)	14(5)	16(5)	0(4)
C8	0.7401(6)	0.9469(5)	0.8925(4)	34(4)	48(5)	57(5)	5(4)	3(4)	-3(4)
C22	0.6541(7)	0.8375(6)	0.7979(3)	60(5)	73(6)	44(4)	8(5)	0(4)	-9(4)
C1'	0.3665(26)	0.9519(18)	0.9082(12)	61(1)					
C2'	0.4314(26)	1.0404(18)	0.9341(12)	61(1)					
C3'	0.4391(26)	1.0321(18)	1.0100(12)	61(1)					
C4'	0.3789(26)	0.9384(18)	1.0309(12)	61(1)					
C5'	0.3340(26)	0.8888(18)	0.9680(12)	61(1)					
C30'	0.4707(26)	1.1407(18)	0.8951(12)	83(4)					
C1	0.3503(7)	0.9179(6)	0.9386(3)	61(1)					
C2	0.4071(7)	1.0161(6)	0.9254(3)	61(1)					
C3	0.4485(7)	1.0566(6)	0.9921(3)	61(1)					
C4	0.4172(7)	0.9835(6)	1.0465(3)	61(1)					
C5	0.3566(7)	0.8978(6)	1.0135(3)	61(1)					
C9	0.8505(4)	0.9726(4)	0.8508(2)	43(2)					
C10	0.9566(4)	0.9139(4)	0.8597(2)	59(2)					
C11	1.0581(4)	0.9344(4)	0.8171(2)	66(2)					
C12	1.0536(4)	1.0135(4)	0.7654(2)	65(2)					
C13	0.9476(4)	1.0722(4)	0.7565(2)	72(2)					
C14	0.8461(4)	1.0518(4)	0.7992(2)	63(2)					
C15	0.8019(6)	1.0326(5)	1.0050(3)	55(2)					
C16	0.7405(4)	1.1276(3)	1.0368(3)	53(2)					
C17	0.7303(4)	1.2189(3)	0.9959(3)	73(3)					
C18	0.6647(4)	1.3042(3)	1.0223(3)	91(3)					
C19	0.6092(4)	1.2982(3)	1.0896(3)	87(3)					
C20	0.6194(4)	1.2069(3)	1.1304(3)	77(3)					
C21	0.6850(4)	1.1216(3)	1.1040(3)	63(2)					
C23	0.7008(8)	0.7252(6)	0.8061(4)	82(3)					
C24	0.5334(4)	0.8462(4)	0.7584(2)	50(2)					
C25	0.4339(4)	0.7836(4)	0.7764(2)	65(2)					
C26	0.3246(4)	0.7941(4)	0.7390(2)	77(3)					
C27	0.3149(4)	0.8671(4)	0.6836(2)	76(3)					
C28	0.4144(4)	0.9297(4)	0.6655(2)	84(3)					
C29	0.5237(4)	0.9192(4)	0.7029(2)	72(3)					
C30	0.4195(10)	1.0726(8)	0.8569(5)	83(4)					

The highest residual electron density was $0.4 \text{ e}^-/\text{\AA}^3$.

Bond lengths, angles, torsional angles are presented in Tables V–VIII, based on the values of the final positional and thermal parameters listed in Tables III and IV. The numbering schemes for the two molecules are shown in Fig. 2 and Fig. 3. The packing of the molecules in the crystal is shown in Fig. 4 and Fig. 5.

Results and Discussion

Bond lengths and angles, as well as the various structural features of the molecules, are as expected

for both compounds, based on previous structural determination of related molecules [1–10, 18].

Common Structural Features

Both compounds consist of square pyramidal $CpMo(CO)_2NCN$ fragments, as shown by the four (Cp ring centroid)–Mo–L angles, all equal to $120 \pm 3^\circ$. The Mo atom lies 1 Å above the basal plane and 2 Å below the Cp ring. The dihedral angle between the basal plane and the Cp plane is 6° . The Mo–N2–C8–N1 chelate rings are almost planar, the Mo atom being less than 0.1 Å away from the N1–C8–N2 plane. When not refined as rigid bodies, all phenyl rings are strictly planar, with all carbon atoms less

TABLE V. Intramolecular Bond Distances (Å)

	MOC PME	MOC P2
Mo–CEN ^a	2.020(8)	2.019(7)
Mo–N1	2.151(5)	2.157(7)
Mo–N2	2.192(5)	2.170(7)
Mo–C6	1.938(7)	1.94(1)
Mo–C7	1.935(8)	1.98(1)
Mo···C8	2.651(8)	2.66(1)
Mo–C1(C1')	2.309(8) 2.47(3)	2.409(7)
Mo–C2(C2')	2.408(8) 2.42(3)	2.415(7)
Mo–C3(C3')	2.434(8) 2.30(3)	2.334(6)
Mo–C4(C4')	2.353(8) 2.28(3)	2.278(7)
Mo–C5(C5')	2.274(8) 2.38(3)	2.326(7)
C6–O6	1.166(7)	1.16(1)
C7–O7	1.160(7)	1.12(1)
C8–C9	1.479(7)	1.47(1)
C8–N1	1.327(8)	1.30(1)
C8–N2	1.317(8)	1.34(1)
N1–C15	1.445(7)	1.50(1)
N2–C22	1.483(8)	1.48(1)
C15–C16	1.507(7)	1.49(1)
C15–C31	–	1.53(1)
C22–C23	1.528(9)	1.50(1)
C22–C24	1.522(7)	1.54(1)
C15–H15	1.08(0) 1.08(0)	1.10(7)
C22–H22	1.08(0)	0.94(6)
CEN···C16 CEN ^a	4.56	4.63
CEN···C24 CEN ^a	5.12	5.12

^aCEN, C16CEN and C24CEN are the ring centroids of, respectively, the cyclopentadienyl ring, C16–C21 phenyl ring and C24–C29 phenyl ring.

TABLE VI. Intramolecular Bond Angles (°)

	MOC PME	MOC P2
N1–Mo–N2	59.5(2)	59.3(3)
N1–Mo–C6	122.3(3)	119.2(4)
N1–Mo–C7	82.0(3)	87.4(4)
N2–Mo–C6	87.3(3)	85.5(4)
N2–Mo–C7	118.8(2)	123.9(4)
C6–Mo–C7	74.8(3)	72.6(4)
CEN–Mo–N1 ^a	118.5(3)	119.1(4)
CEN–Mo–N2 ^a	120.5(3)	118.6(4)
CEN–Mo–C6 ^a	119.0(3)	121.2(4)
CEN–Mo–C7 ^a	119.4(3)	116.9(4)
Mo–N1–C8	96.5(4)	97.2(6)
Mo–N1–C15	138.4(4)	141.5(6)
C8–N1–C15	125.0(6)	121.3(8)
Mo–N2–C8	94.9(4)	95.3(6)
Mo–N2–C22	142.6(5)	142.6(6)
C8–N2–C15	121.0(6)	119.5(8)
Mo–C6–O1(O6)	176.8(8)	174(1)
Mo–C7–O2(O7)	178.1(7)	176(1)
N1–C8–N2	109.2(6)	108.1(8)
N1–C8–C9	125.8(6)	126.3(8)
N2–C8–C9	125.0(6)	125.6(8)
N1–C15–C16	111.7(5)	110.5(8)

TABLE VI. (continued)

	MOC PME	MOC P2
N1–C15–C31	–	109.6(8)
N1–C15–H15	108.9(3)	110(4)
N2–C22–C23	110.7(6)	113.7(9)
N2–C22–C24	111.0(5)	110.4(8)
N2–C22–H22	109.3(4)	109(4)

^aCEN is the Cp ring centroid.

TABLE VII. Torsion Angles (°)

	MOC PME		MOC P2	
N1–Mo–CEN ^a	–C(3)	–10.3	–C(1)	–10.1
N1–Mo–CEN–C2		61.9		62.0
N2–Mo–CEN–C2		–7.6		–6.8
N2–Mo–CEN	–C(1)	64.2	–C(3)	65.1
C6–Mo–CEN	–C(1)	–41.1	–C(3)	–38.1
C6–Mo–CEN	–C(5)	31.0	–C(4)	33.9
C7–Mo–CEN–C4		14.9		–51.2
C7–Mo–CEN–C5		–57.1		20.9
Mo–N2–C22–C24		59.1		64.8
Mo–N1–C15–C16		–60.1		–48.4
N1–C8–C9–C14		–105.0		82.6
N2–C8–C9–C14		–77.7		–97.9
N1–C15–C16–C21		91.9		–98.5
N2–C15–C24–C25		–77.1		–74.3
H22–C22–N2–Mo		175.1		–176.3
H22–C22–N2–C8		–23.5		–20.2
H15–C15–N1–Mo		179.5		–168.4
H15–C15–N1–C8		4.8		9.8
N1–Mo–CEN'–C3'		–44.3		
N1–Mo–CEN'–C2'		27.4		
N2–Mo–CEN'–C2'		–40.1		
N2–Mo–CEN'–C1'		32.1		
C6–Mo–CEN'–C1'		–67.7		
C6–Mo–CEN'–C5'		4.3		
C7–Mo–CEN'–C3'		58.6		
C7–Mo–CEN'–C4'		–13.6		

^aCEN and CEN' are, respectively, the ring centroids of the two Cp images.

than 3σ away from the least squares planes. The exocyclic phenyl groups [C9–C14] are almost perpendicular to the N1–C8–N2 ligand planes (the interplanar angles in MOC PME and MOC P2 being 101° and 98°, respectively). The two fragments are thus not conjugated, and the C8–C9 bond lengths (see Table V) are equal to 1.477 Å, as expected [17] for a Csp²–Csp² single bond. In both compounds, H15 and H22 lie close to the plane defined by N1, C8, N2 and the side phenyls are up and face the apical Cp ring. These are common features to all preferred diastereoisomers.

TABLE VIII. Least Squares Planes and Deviations of Atoms from these Planes

Plane 1: based on C1 through C5			
MOCPME: $(0.8755)x + (-0.4657)y + (-0.1289)z - (-4.331) = 0$		Mo	2.014 Å
MOCP2: $(-0.6066)x + (0.4922)y + (-0.6243)z - (-8.677) = 0$		Mo	2.014 Å
Plane 2: based on N1, N2, C8			
MOCPME: $(-0.4608)x + (0.8355)y + (-0.2994)z - (1.351) = 0$		Mo	-0.082 Å
MOCP2: $(0.7720)x + (-0.6354)y + (-0.0157)z - (0.020) = 0$		Mo	-0.055 Å
Plane 3: based on C9 through C14			
MOCPME: $(-0.3282)x + (-0.6605)y + (-0.6753)z - (-21.963) = 0$			
MOCP2: $(0.5205)x + (0.8538)y + (-0.0079)z - (2.725) = 0$			
Plane 4: based on C16 through C21			
MOCPME: $(-0.8305)x + (-0.3583)y + (-0.4265)z - (-20.148) = 0$			
MOCP2: $(-0.7811)x + (-0.4536)y + (-0.4292)z - (-3.762) = 0$			
Plane 5: based on C24 through C29			
MOCPME: $(0.3027)x + (-0.6923)y + (-0.6550)z - (-14.945) = 0$			
MOCP2: $(-0.0088)x + (0.9391)y - (-0.3436)z - (1.093) = 0$			
Plane 6: based on N1, N2, C6 and C7			
MOCPME: $(0.8289)x + (-0.5550)y + (-0.0698)z - (-1.545) = 0$		Mo	-0.998 Å
MOCP2: $(-0.6648)x + (0.5169)y + (-0.5393)z - (-4.838) = 0$		Mo	-0.992 Å
Plane 1	Plane 2	MOCPME	MOCP2
1	4	120°	59°
1	5	48°	47°
1	6	7°	6°
2	3	101°	98°

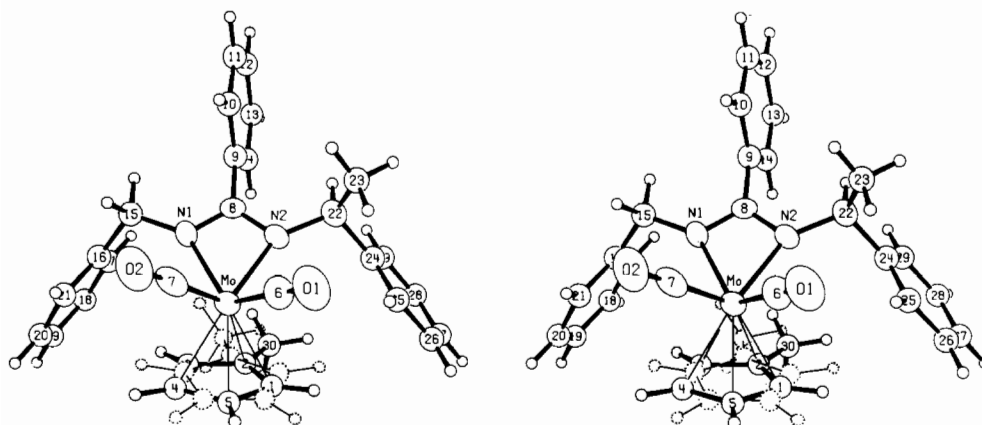


Fig. 3. Stereoscopic view of the molecule of MOCPME showing the atom labelling scheme. The minor Cp image is depicted as dotted lines.

Orientation of the Cp Ring

It has invariably been found [18] that in *cis* $Cp(CO)_2ML_1L_2$ complexes, the minimum $C(Cp)-(ring\ centroid)-M-L$ torsion angle relates a Cp carbon with some ligand other than carbonyl. MOCP2 and the higher occupancy (80%) Cp ring in MOCPME are no exception to this finding, and they have the same orientation with respect to the basal plane

ligands, as shown by the similar $C(Cp)-(ring\ centroid)-M-L$ torsion angles for both compounds. However, for the minor (20%) image of the Cp ring in MOCPME, one carbon is found to eclipse one of the carbonyl groups. The rotation of the Cp from the major to the minor image clearly puts the methyl of the Cp away from both side phenyls, but we do not believe this is the driving force in disordering

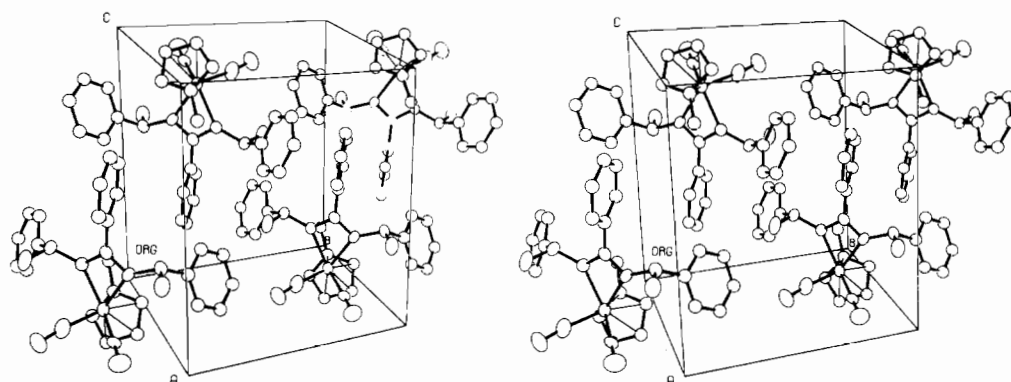


Fig. 4. Stereoscopic view of the molecular packing of MOCP2 in the crystal lattice, with hydrogens omitted for clarity.

the Cp, since a similar situation, with a major Cp image eclipsing nitrogen and a minor Cp image eclipsing carbonyls has already been reported [8] for a benzamidine with a non-methylated Cp.

Absolute Configuration and Optical Activity

MOCPME

The C22 site has a chirality of (*S*). The priority sequence $\eta^5\text{-C}_5\text{H}_5 > \text{N-CH}(\text{CH}_3)\text{C}_6\text{H}_5 > \text{N-CH}_2\text{C}_6\text{H}_5 > \text{CO}$ may be used to assign the chirality indicator (*R*) at the Mo site. The chirality at Mo is correlated to the sign of the rotational amplitude of the CD spectra in the region of 578 nm [8]. It is reasonable not to expect any drastic changes in this correlation due to the addition of a methyl on the Cp ring. We can thus predict this (*S*;C)(*R*;Mo) diastereoisomer CD spectra to have a (–) rotational amplitude around 578 nm.

MOCP2

The C22 and C15 sites have a respective chirality of (*S*) and (*R*) in the (*x, y, z*) symmetry position;

of (*R*) and (*S*) in the ($\bar{x}, \bar{y}, \bar{z}$) symmetry position. The two molecules in the unit cell, mirror images are not superimposable because of conformational effects: in one of the molecules (depicted in Fig. 3.) the methyl on the Cp points at the (*S*) carbon, in the other molecule it points at the (*R*) carbon. In solution, however, it is possible to bring the molecule to a conformation where it has a mirror plane. Even if this conformation is unstable the two 'conformational enantiomers' will always be present in the solution: it will not be optically active.

Comparison of MOCPME, MOCP2 and BENZ Ia

Benz Ia is one of the independent molecules of BENZ I. BENZ I [8] is a benzamidine differing from MOCPME only by its non-methylated Cp. Comparison of MOCPME and MOCP2 against Benz Ia should allow us to assess the conformational effects due to the methyl on the Cp. Figures 6 and 7 provide a visual comparison of conformational differences between (MOCPME and BENZ Ia) and (MOCPME and MOCP2), respectively. The best fit between molecules was produced [19] using

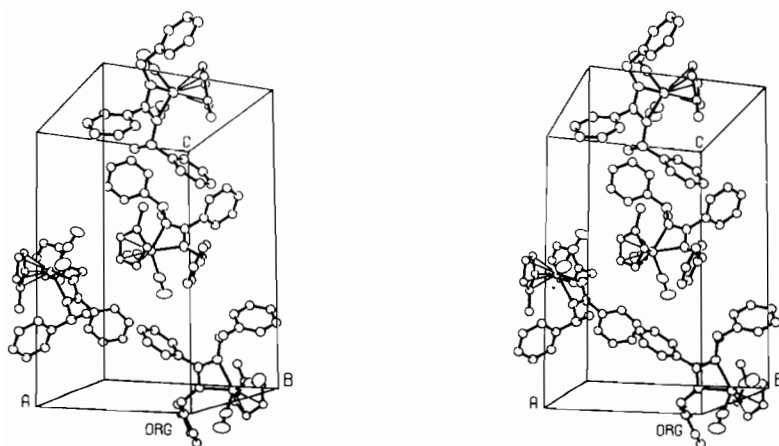


Fig. 5. Stereoscopic view of the molecular packing of MOCPME in the crystal lattice, with hydrogens omitted for clarity.

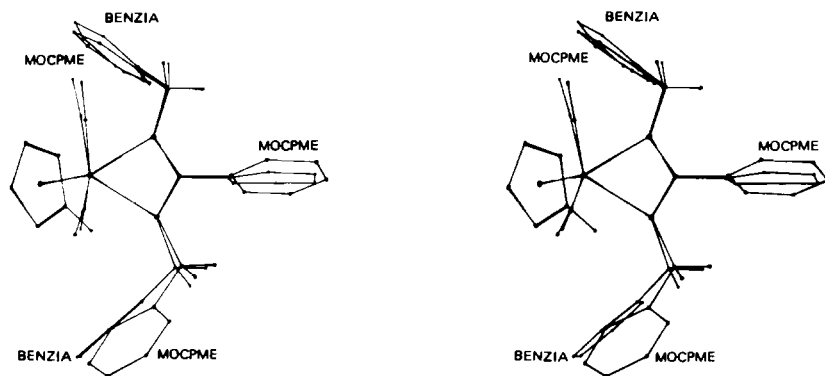


Fig. 6. BMFIT [19] diagram showing Benz I and MOC PME.

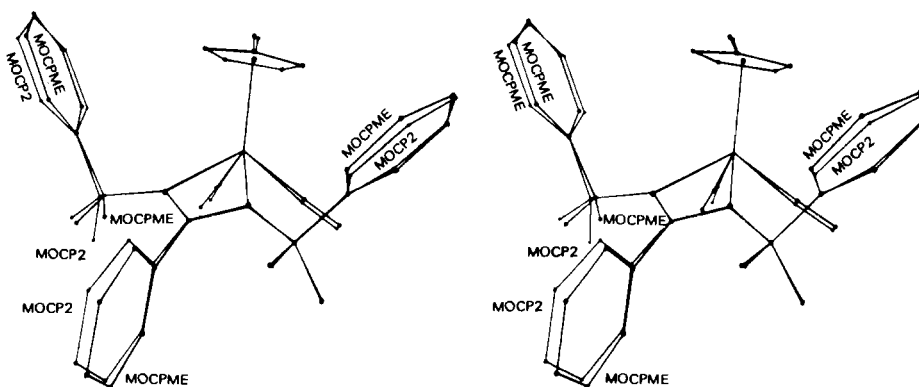


Fig. 7. BMFIT [19] diagram showing MOC P2 and MOC PME.

the Mo atom, the Cp ring centroid, N1 and N2. Distances between corresponding atoms were then calculated.

The fit between the Cp rings in the three compounds is excellent, with the Cps less than 0.06 Å from one another, and thus in the very same conformation with respect to the basal plane ligands. The fit between MOC P2 and MOC PME is very good, with the maximum distance between corresponding atoms less than 0.2 Å for the C24–C29 ring, less than 0.3 Å for C9–C14 ring and less than 0.4 Å for the C16–C21 ring. For this last ring, the deviation can be explained by the additional CH_3 group on C15 in MOC P2 and the concomitantly increased H15–C15–N1–C8 torsion angle. In spite of the large area over which packing forces can be exerted on the phenyl rings, they clearly are not determining the conformation of these molecules.

The fit between MOC PME and BENZ Ia is also very good for the C16–C21 ring. The C9–C14 ring has pivoted into a different conformation, the maximum distance being now 0.8 Å, but the largest deviation occurs with the C24–C29 ring, two atoms even having no match at less than 1 Å. The (Cp ring

centroid)–(phenyl C24–C29 ring centroid) distance is now, in MOC PME and MOC P2, 0.5 Å longer than the (Cp ring centroid)–(phenyl C16–C21 ring centroid). This positional difference of the C24–C29 ring between MOC P2 (MOC PME) and BENZ Ia is obviously due to the methyl on the Cp. Interestingly, although the methyl caused the C24–C29 ring to move away, the preferred orientation of the Cp was not affected by the phenyl–methyl interaction. This shifting away of the C24–C29 ring in MOC PME (or MOC P2) as compared to BENZ Ia call for one more remark: although the C24–C29 ring is now further away from Cp, and although the interaction between phenyl and Cp takes place ‘through’ the methyl (the methyl being positioned in between Cp and phenyl), the preferred diastereoisomer is still the one that has the phenyl up and facing the Cp. This interaction between phenyl and Cp will be dealt with at length in the next paragraph.

Interaction Between the Side Phenyl Ring and the Apical Cp Group

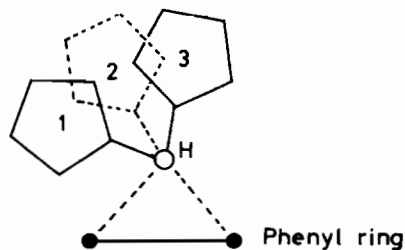
The orientation of the phenyl ring with respect to the cyclopentadiene ring has been described

briefly in previous studies as [4, 6, 8] 'The phenyl facing the apical Cp group'. We will now study and describe this orientation in a more detailed and precise way. In the following, we will say that the phenyl ring is 'faced' by one hydrogen when:

(a) the 6 H...C(phenyl) distances are within 10% of one another;

(b) the H...(phenyl ring centroid) distance is shorter than any of the above.

This amounts to saying that the hydrogen lies almost on the line perpendicular to the phenyl ring passing through its centroid. This conformation allows the Cp hydrogen to come as close as possible to the phenyl ring while maximizing the sum of the van der Waals attractive interactions with the carbons of the phenyl ring. From Table IX, which gives the contact distances between hydrogens and phenyl rings in MOCPME and MOCP2, it is clear that the two phenyl rings C16-C21 and C24-C29 orient themselves to be 'faced' by one H of the methyl cyclopentadienyl group. In both compounds C16-C21 interacts with one ring H, but at this point it is important to note that C24-C29 interacts with one of the methyl hydrogens, with contact distances only slightly longer than the C16-C21...H (ring) contact distances. In MOCPME, the second Cp image has no H 'facing' the phenyl rings. Since the occupancy of Cp is only 20%, it is not surprising that H(Cp')...phenyl interactions are not favored in MOCPME. Table IX also gives intermolecular H...phenyl 'facing' interactions. In MOCPME, the H involved is a phenyl hydrogen, while in MOCP2 it is a methyl hydrogen. However, the preceding remarks on the orientation of phenyls with respect to hydrogens do not fix the orientation of the Cp rings themselves, as illustrated in the Figure:



Although orientations 1, 2, 3 of the phenyl ring with respect to the cyclopentadienyl ring are different, the phenyl ring is still 'faced' by the same hydrogen. The angles θ_1 and θ_2 , described in Fig. 8, between the edge of the Cp and the phenyl ring can be used as a measure of these orientations. Geometry considerations require that $\theta_1 + \theta_2 = 72^\circ$, so we choose as a measure θ_i ($i = 1$ or 2), whichever is smallest. Thus, θ_i will always be $0 \leq \theta_i \leq 36^\circ$. Table X gives the value of θ_i for various benzamides.

TABLE IX. Inter- and Intra-molecular Contacts for 'Facing' Hydrogens in MOCPME and MOCP2

Intra/intermolecular contacts (H involved in interaction; ring involved in interaction)	MOCPME		MOCP2	
	Intramolecular		Intermolecular	
	H3; C16-C21	H3'; C16-C21	H19; C9-C14	H1; C16-C21
H...C1	2.82	2.88	3.25	2.85
H...C2	2.88	3.32	3.15	2.86
H...C3	3.00	3.44	2.95	3.06
H...C4	3.06	3.13	2.86	3.18
H...C5	3.00	2.66	2.95	3.20
H...C6	2.88	2.51	3.15	3.00
H...(ring centroid)	2.60	2.67	2.72	2.69
		H30A; C24-C29	H30A; C24-C29	
		2.89	2.94	
		3.18	2.59	
		3.39	2.79	
		3.32	3.29	
		3.04	>3.5	
		2.81	3.42	
		2.78	2.79	
			H23C; C9-C14	
			3.00	
			3.06	
			3.17	
			3.16	
			3.15	
			3.22	
			3.00	
			2.75	

TABLE X. Angle θ^a between the edge of the Cp and the Phenyl Ring in Mo-benzamidines Compounds

Compound	Benz Ia	Benz Ib	Benz II		Benz III		MOCPME		MOCP2
			θ	θ' b	θ	θ' b	θ	θ' b	
θ for first phenyl ring	1	34	8	17	7	9	9	31	1
θ for second phenyl ring	17	13					30 ^c	12	32 ^c

^a θ is the smallest of the two angles θ_1 and θ_2 defined in Fig. 8. ^b θ' is the angle with the second Cp image, when Cp is disordered. ^ca methyl is positioned in between Cp and phenyl.

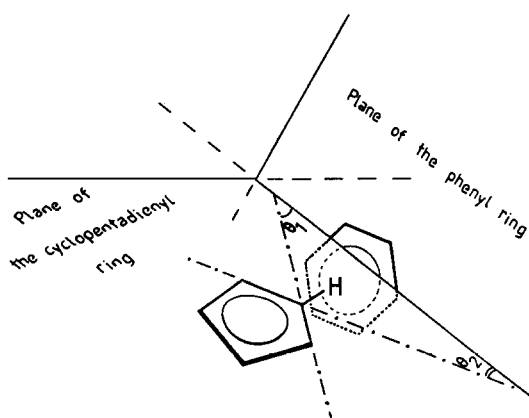


Fig. 8. The two angles θ_1 and θ_2 between the edge of the Cp and the phenyl ring plane. ($\theta_1 + \theta_2 = 72^\circ$).

Those values cover the entire range of 0° to 36° , which shows that the relative orientation of the two rings (as described by θ_i) has no role in the preferred conformation of those molecules, when the phenyl is close to the Cp. Thus, we reach the conclusion that in preferred diastereoisomers, the attractive interaction noted [4–8] between the phenyl and the Cp is more a hydrogen-to-ring interaction than a ring-to-ring interaction. The side chain phenyls orient themselves to maximize the attractive van der Waals forces

between one Cp hydrogen and the six (phenyl) carbons and thus adopt a 'H faced' position. This conclusion has been checked and found to explain the differences noted between Benz Ia and Benz Ib, the two independent molecules in the crystal of BENZ I [8]. Benz Ia and Ib differ in the orientation of the Cp, eclipsing N1 in Ia, eclipsing N2 in Ib, as shown in Fig. 9 (from ref. 8).

The contact distances between the Cp hydrogens and the phenyl rings for Ia and Ib are presented in Table XI. The C16–C21 ring, 'faced' by H3 in Ia, would not be 'faced' by a hydrogen in Ib because of the rotation of the Cp. Therefore, it rotates in Ib to be 'faced' by H4'. This motion can clearly be seen in Fig. 9. The C24–C29 ring in Ib is 'faced' by H2'. In Ia, the C24–C29 ring could move to be 'faced' either by H1 or H2. But the motion towards H1 would increase significantly the C8–N2–C22–H22 torsion angle, which is known to be unfavorable. On the other hand, the move to be 'faced' by H2 would decrease the same torsion angle, thus increasing the $CH_3 \cdots CO$ steric interaction. That is why C24–C29 adopts an intermediate position in which the phenyl carbons are within van der Waals attraction range of both H1 and H2. This position is approximately the same as that for C24–C29 in Ib.

We thus see that the orientation of the phenyl rings with respect to the Cp can be explained by

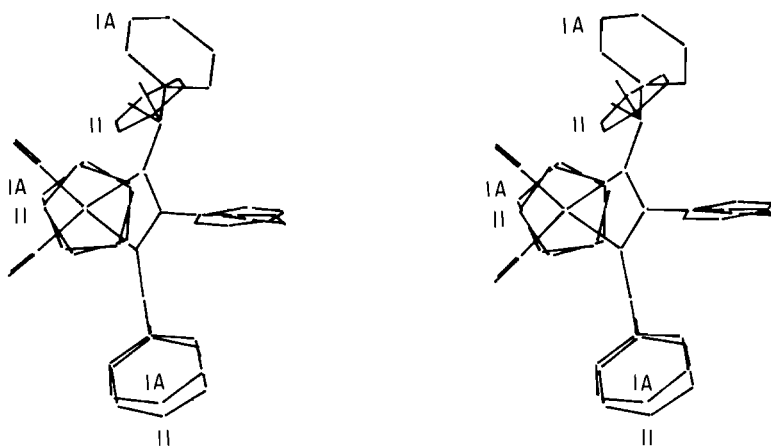


Fig. 9. BMFIT [19] diagram showing Benz Ia and Ib (from ref 8).

TABLE XI. Intramolecular Contacts between Cp Hydrogens and Side Phenyls in Benz Ia and Benz Ib

	Ia	Ib	
Ring C16–C21			
H involved in interaction	H3	H4'	
H...C1	2.93	3.25	
H...C2	3.18	3.39	
H...C3	3.27	3.62	
H...C4	3.14	3.73	
H...C5	2.88	3.54	
H...C6	2.78	3.34	
H...(ring centroid)	2.71	3.26	
Ring C24–C29			
H involved in interaction	H1	H2	H2'
H...C1	3.18	3.21	2.91
H...C2	3.61	2.83	2.90
H...C3	3.65	3.21	3.04
H...C4	3.28	3.84	3.18
H...C5	2.85	4.08	3.18
H...C6	2.78	3.84	3.04
H...(ring centroid)	2.94	3.26	2.76

intramolecular forces, and is unnecessary to invoke intermolecular packing forces to arrive at a rational explanation for the conformation effects observed in these systems.

Comparison with Solution Data

MOC PME, BENZ I and their nonpreferred diastereoisomers have been studied in solution [20]. The diastereoisomeric ratios (preferred isomer/non preferred isomer) do not differ significantly for the two compounds, being 67/33 and 70/30, respectively, in acetone at 70 °C. The cyclopentadiene ring in BENZ I rotates freely, but the rotation is restricted when it is methylated, as shown by the multiplet obtained in ¹H NMR for MOC PME. For both compounds the resonances of the cyclopentadienyl protons are shifted by 0.7 ppm downfield as one goes from the preferred to the non-preferred diastereoisomer: the anisotropy induced, in the preferred diastereoisomer, by the two phenyl rings up and close to the cyclopentadienyl ring is larger than in the non-preferred diastereoisomer, where one phenyl ring only interacts with the Cp protons. The methyl (of the Cp) resonance is also shifted downfield (by 0.4 ppm): the methyl is thus in the field created by the phenyls in solution as it is in the solid state. Methyla-

tion of the cyclopentadienyl ring is thus found not to affect the behavior of these compounds, as demonstrated by the similar diastereoisomeric ratios and NMR data: solution and crystal data are in close agreement, again showing that the conformations of MOC PME and BENZ I, as well as those of their non-preferred diastereoisomers, are not artifacts of the solid state.

Acknowledgements

We thank the Robert A. Welch Foundation for research support (grant E-594). We also thank Professor Henri Brunner for the crystals used in this study.

References

- 1 M. G. Reisner, I. Bernal, H. Brunner and J. Wachter, *J. Organomet. Chem.*, **137**, 329 (1977).
- 2 M. G. Reisner and I. Bernal, *J. Organomet. Chem.*, **220**, 55 (1981).
- 3 M. W. Creswick and I. Bernal, *Inorg. Chim. Acta*, **57**, 171 (1982).
- 4 H. Brunner, G. Agrifoglio, I. Bernal and M. W. Creswick, *Angew. Chem.*, **92**, 645 (1980); *Angew. Chem., Int. Ed. Engl.*, **19**, 641 (1980).
- 5 H. Brunner, J. Lukassek and G. Agrifoglio, *J. Organomet. Chem.*, **195**, 63 (1980).
- 6 I. Bernal, M. W. Creswick, H. Brunner and G. Agrifoglio, *J. Organomet. Chem.*, **198**, C4 (1980).
- 7 H. Brunner and G. Agrifoglio, *J. Organomet. Chem.*, **202**, C43 (1980).
- 8 M. W. Creswick and I. Bernal, *Inorg. Chim. Acta*, **74**, 241 (1983).
- 9 H. Brunner, *Acc. Chem. Res.*, **12**, 250 (1979).
- 10 H. Brunner, G. Agrifoglio, R. Benn and A. Rufinska, *J. Organomet. Chem.*, **217**, 365 (1981).
- 11 D. T. Cromer and J. B. Mann, *Acta Crystallogr., Sect. A.*, **24**, 321 (1968).
- 12 R. F. Stewart, E. R. Davidson and W. T. Simpson, *J. Chem. Phys.*, **42**, 3175 (1965).
- 13 D. T. Cromer and D. Liberman, *J. Chem. Phys.*, **53**, 1891 (1970).
- 14 J. M. Bijvoet, A. F. Peerdeman and A. J. Van Bommel, *Nature (London)*, **168**, 271 (1951).
- 15 R. S. Cahn, C. Ingold and V. Prelog, *Angew. Chem.*, **78**, 413 (1966).
- 16 K. Stanley and M. C. Baird, *J. Am. Chem. Soc.*, **97**, 6599 (1975).
- 17 D. W. J. Cruikshank and R. A. Sparks, *Proc. R. Soc. London, Ser. A*, **270** (1960).
- 18 M. W. Creswick, *Ph.D. Dissertation*, University of Houston, 1980.
- 19 L.-K. Liu, 'Program BMFIT', University of Texas, Austin, 1977 (based upon S. C. Nyburg, *Acta Crystallogr., Sect. B.*, **30**, 251 (1974)).
- 20 H. Brunner and B. Schönhammer, *Z. Naturforsch., Teil B.*, **38**, 852 (1983).